



저작자표시-비영리-변경금지 2.0 대한민국

이용자는 아래의 조건을 따르는 경우에 한하여 자유롭게

- 이 저작물을 복제, 배포, 전송, 전시, 공연 및 방송할 수 있습니다.

다음과 같은 조건을 따라야 합니다:



저작자표시. 귀하는 원저작자를 표시하여야 합니다.



비영리. 귀하는 이 저작물을 영리 목적으로 이용할 수 없습니다.



변경금지. 귀하는 이 저작물을 개작, 변형 또는 가공할 수 없습니다.

- 귀하는, 이 저작물의 재이용이나 배포의 경우, 이 저작물에 적용된 이용허락조건을 명확하게 나타내어야 합니다.
- 저작권자로부터 별도의 허가를 받으면 이러한 조건들은 적용되지 않습니다.

저작권법에 따른 이용자의 권리는 위의 내용에 의하여 영향을 받지 않습니다.

이것은 [이용허락규약\(Legal Code\)](#)을 이해하기 쉽게 요약한 것입니다.

[Disclaimer](#)

**Thesis for the Degree of Master of Engineering**

**Effects of Thermal Treatment on Physical  
Properties of Edible Calcium Alginate Gel  
Beads**



**by**

**Seonghui Kim**

**Department of Food Science & Technology**

**The Graduate School**

**Pukyong National University**

**February 21, 2020**

# **Effects of Thermal Treatment on Physical Properties of Edible Calcium Alginate Gel Beads**

**열처리가 식용 Calcium Alginate Gel Beads의  
물리적 특성에 미치는 영향**

**Advisor: Prof. Seon-Bong Kim**

**by**

**Seonghui Kim**

**A thesis submitted in partial fulfillment of the requirements  
for the degree of**

**Master of Engineering**

**in Department of Food Science & Technology, the Graduate School,  
Pukyong National University**

**February, 2020**

# Effects of Thermal Treatment on Physical Properties of Edible Calcium

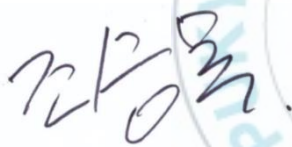
## Alginate Gel Beads

A dissertation

by

Seonghui Kim

Approved by



(Chairman) Suengmok Cho, Ph. D.



(Member) Young-Mog Kim, Ph. D.



(Member) Seon-Bong Kim Ph. D.

February 21, 2020

# Contents

<b>Contents</b> .....	<b>i</b>
<b>List of Tables</b> .....	<b>iii</b>
<b>List of Figures</b> .....	<b>v</b>
<b>Abstract</b> .....	<b>vi</b>
<b>Introduction</b> .....	<b>1</b>
<b>Materials and Methods</b> .....	<b>3</b>
1. Materials.....	3
2. Preparation of CAG beads.....	3
3. Measurement of size and sphericity of CAG .....	5
4. Measurement of rupture strength .....	5
5. Experimental design.....	5
6. Data analysis and optimization .....	8
7. Scanning electron microscopy (SEM).....	8
8. Weight and water contents of the CAG beads.....	9
9. Measurement of density .....	9
<b>Results and Discussion</b> .....	<b>10</b>
1. Diagnostic checking of the fitted models .....	10
2. Response surface plots and the effect of factors .....	14
3. Microstructure .....	19
4. Optimal conditions and verification.....	24
<b>Conclusions</b> .....	<b>28</b>
<b>References</b> .....	<b>29</b>

**Publications and Presentations** ..... 33  
**Acknowledgments** ..... 34



## List of Tables

Table 1. Experimental range and values of independent variables in the central composite design for monitoring the effects of thermal treatment on physical properties of CAG beads.....	7
Table 2. Central composite design matrix and values of dependent variables for monitoring the effects of thermal treatment on physical properties of CAG beads .....	11
Table 3. Response surface model equations for monitoring the effects of thermal treatment on physical properties of CAG beads .....	12
Table 4. Analysis of variance for dependent variables.....	13
Table 5. Estimated coefficients of the fitted quadratic polynomial equations for dependent variables based on the t-statistic .....	17
Table 6. Density ( $\text{g/cm}^3$ ) of CAG beads .....	21
Table 7. The rupture strength, size, and sphericity of before heat treatment CAG beads. ....	25

Table 8. Response optimization for processing a heated CAG beads similar result to non-heated CAG beads conditions.....  
..... **26**

Table 9. Experimental and predicted results of verification under optimized conditions.....  
..... **27**



## List of Figures

Figure 1. Simple schematic diagram for preparation calcium alginate gel (CAG) beads using a single nozzle .....	<b>4</b>
Figure 2. Three-dimensional response surface plots for rupture strength (a), size (b), and sphericity (c). X <sub>1</sub> ; Heating temperature (°C), X <sub>2</sub> ; Heating time (min) .....	<b>18</b>
Figure 3. Digital microscope (left), and SEM (right) photographs of CAG beads frozen in liquid nitrogen and freeze-dried: (a) before heat treatment CAG bead; (b) CAG beads were heated at 40 °C; (c) CAG beads were heated at 70 °C; (d) CAG beads were heated at 100 °C. Magnification of the images are 40×, 500×, and 2500×.....	<b>20</b>
Figure 4. Correlation between weight (mg) and size (mm), water content (%) and size (mm) at 5 min; and weight (mg) and size (mm), water content (%) and size (mm) at 32.5 min .....	<b>23</b>

# 열처리가 식용 Calcium Alginate Gel Beads의 물리적 특성에 미치는 영향

김성희

부경대학교 대학원 식품공학과

## 요약

Calcium alginate gel (CAG)은 인조식품 및 모조식품 개발을 위해 광범위하게 조사되어 왔으나 열안정성에 관한 연구는 거의 이루어지지 않았다. 본 연구는 열처리 중 CAG beads의 물리적 특성 변화를 통계적 기법인 반응표면분석법(response surface methodology, RSM)을 이용하여 모니터링했다. 독립변수로는 가열온도( $X_1$ , 40–100 °C) 및 가열시간( $X_2$ , 5–60 min), 종속변수로는 파열강도( $Y_1$ , kPa), 직경( $Y_2$ ,  $\mu\text{m}$ ) 및 구형도( $Y_3$ , %)을 설정하였다. 가열온도( $X_1$ )는 파열강도( $Y_1$ )와 직경( $Y_2$ )에 상당한 영향을 미친 독립변수였다. 파열강도( $Y_1$ )는 가열온도( $X_1$ )가 증가함에 따라 증가하였으며 직경( $Y_2$ )은 감소하였다. 모든 조건에서, 구형도( $Y_3$ )의 값은 94% 이상이 었다. 미세구조를 주사전자현미경으로 관찰한 결과는 열처리에 의한 밀집된 다공성 구조에 의해 CAG beads의 파열강도( $Y_1$ )가 증가한다는 것을 보여주었다. 또한 열처리시 발생하는 syneresis에 의한 수분함량 감소는 CAG beads의 밀집된 다공성 구조를 만드는 것으로 판단되었다. 본 연구결과는 CAG

beads를 이용하여 식품을 요리하거나 살균하는데 유용한 정보를 제공한다.  
또한 열처리가 적용되어 파열강도 ( $Y_1$ )가 높은 단단한 CAG beads를  
생산할 수 있다.



## Introduction

Alginate is a linear anionic polysaccharide derived from brown seaweeds and is composed of (1-4)-linked  $\beta$ -D-mannuronic (M) and  $\alpha$ -L-guluronic acid (G) residues [1,2]. It can form gel through cross linking with divalent cations, forming an egg-box structure [1,3]. Among divalent cations, calcium is the most commonly used cation for ionotropic gelation of alginate [1]. Calcium alginate gel (CAG) is easily produced by extrusion methods, by dripping the alginate solution into a calcium ion solution [4]. CAG has been investigated as a thickener, stabilizer, and restructuring agent in food processing because of its unique gelling abilities [5]. Furthermore, CAG has been applied in cell encapsulation, drug delivery and tissue engineering [6].

In recent years, there has been an increasing interest in CAG as a biomaterial for making artificial or imitative foods. Some researchers have studied the optimization of the processing of fish roe [7,8] and effects of the physicochemical parameters of cooked rice [9] analogs using CAG. Many studies have focused on optimizing the processing conditions, such as concentration of the alginate or calcium and gelation time. To date, little attention has been paid to the thermal stability of CAG. In the food industry, foods prepared with CAG are subjected to various forms of heat treatment. For example, food safety issues require thermal processes for sterilization of the CAG; moreover, CAG foods may be heated for cooking or manufacturing. During thermal treatments, CAG's physical properties undergo changes; however, no information can be found. The physical properties of alginate gels are used to enhance food product quality and

stability during storage [10,11]. Therefore, it is important to investigate the effects of thermal treatment on physical property changes in CAG, for application and processing of CAG-based foods.

This study aimed to understand the effects of heat treatment on the physical properties of CAG beads for its application to fish roe analogs. The central composite design (CCD) of response surface methodology (RSM) was adopted to monitor the effects of heat treatment. RSM is a statistical procedure frequently used for optimization and monitoring of food processes. The basic principle of RSM is to describe model equations defining the effect of test variables on responses and determine interrelationships among test variables in any response [12]. The CCD was reported for designing the experiment, to create a model, and to optimize the process variables with sensory and hedonic properties of food products [13]. Heating temperature and time were chosen as the independent variables. Rupture strength, size, and sphericity were measured to explore the physical property changes of the CAG beads after heat treatment. Furthermore, microstructures were analyzed using scanning electron microscopy.

# Materials and Methods

## 1. Materials

Sodium alginate (Junsei Chemical Co., Ltd., Tokyo, Japan) and calcium lactate (Daejung chemical & metal Co., Ltd., Siheung, Korea) were used as the functional materials for CAG beads. All chemicals and reagents used in this study were of an analytical grade.

## 2. Preparation of CAG beads

A sodium alginate solution (2.57%, w/v) was dropped through a single nozzle 20G (inner diameter: 0.60 mm, outer diameter: 0.90 mm) using a peristaltic pump (Cassette tube pump SMP-23, Eyela, Tokyo, Japan) into a calcium lactate solution (1.52%, w/v). The stirring speed of calcium lactate solution (250 mL) in the reactor (500 mL) was 300 rpm. The distance between the nozzle tip and the surface of the calcium lactate solution was 8 cm. The allowed gelation time was 20 min. The CAG beads were rinsed with distilled water to remove any remaining calcium lactate. A schematic diagram for preparation of CAG beads is shown in Figure 1.

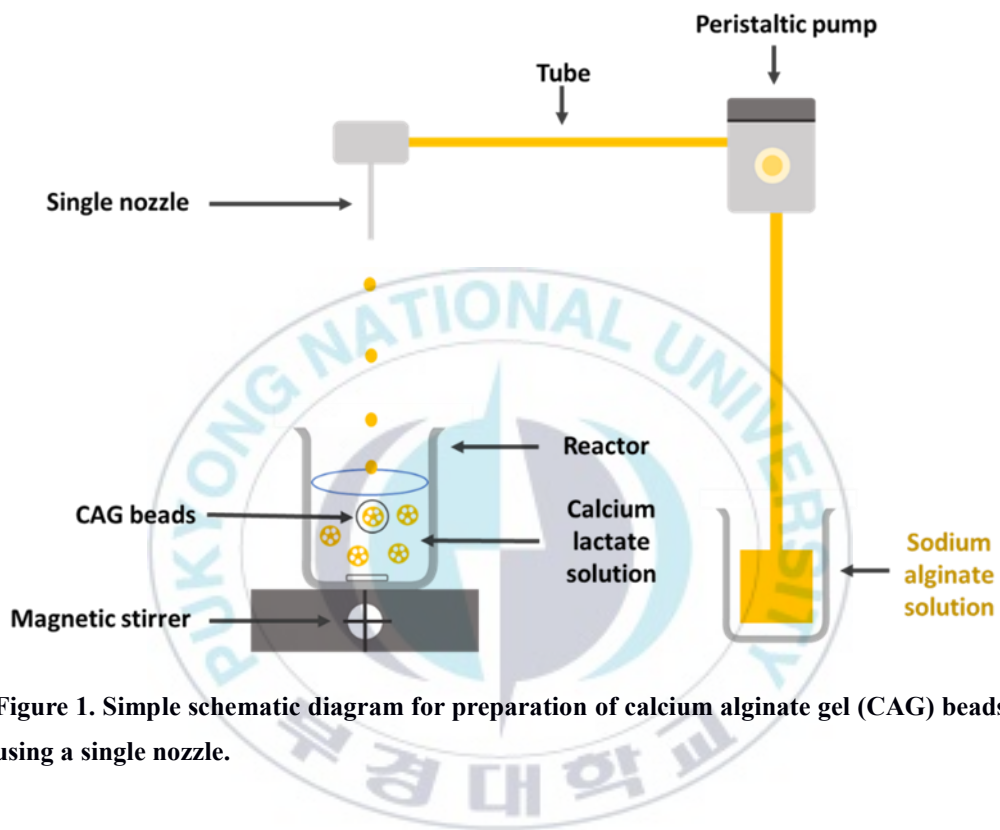


Figure 1. Simple schematic diagram for preparation of calcium alginate gel (CAG) beads using a single nozzle.

### **3. Measurement of size and sphericity of CAG**

CAG beads sizes were measured by a stereomicroscope (Olympus SZX16; Tokyo, Japan) and were represented as diameter (mm). Sphericity (%) was determined by the percent ratio of the minor diameter to major diameter, obtained from the size measurements; five beads were randomly selected from each experimental condition for measurement.

### **4. Measurement of rupture strength**

The rupture strength was measured using a rheometer (Model CR-100D, Sun Scientific Co., Ltd., Tokyo, Japan) with the following conditions: plunger diameter, 25 mm; penetration speed, 80 mm/min; adaptor area, 4.91 cm<sup>2</sup>; and load cell force, 0.1 kN. Five samples were measured for each experiment.

### **5. Experimental design**

To monitor the effects of heat treatment on the physical properties of the CAG beads, a central composite design (CCD) was adopted in the optimization of the CAG beads. CCD in this design comprises 2<sup>2</sup> factorial points, 4 axial points ( $\alpha = 1.414$ ), with 3 replicates of the central points. Heating temperature ( $X_1$ , °C) and time ( $X_2$ , min) were chosen as independent variables. The range and center point values of the two independent variables were based on the results of preliminary experiments (Table 1). The dependent variables were rupture strength ( $Y_1$ , kPa), size ( $Y_2$ ,  $\mu\text{m}$ ), and sphericity

( $Y_3$ , %), indicating physical characteristics of the CAG beads. The experiments were randomized to minimize the effects of unexpected variability in the observed responses.



**Table 1. Experimental range and values of independent variables in the central composite design for monitoring the effects of thermal treatment on physical properties of CAG beads.**

Independent variables	Symbol	Range and levels				
		-1.414	-1	0	+1	+1.414
Heating temperature (°C)	X <sub>1</sub>	40	49	70	91	100
Heating time (min)	X <sub>2</sub>	5	13	33	52	60

## 6. Data analysis and optimization

Using the response surface methodology of MINITAB statistical software (Version 16, Minitab Inc., Harrisburg, PA, USA), Equation (1) was used to fit results [14].

$$Y = \beta_0 + \sum_{i=1}^4 \beta_i X_i + \sum_{i=1}^4 \beta_{ii} X_i^2 + \sum_{i=1}^3 \sum_{j=i+1}^4 \beta_{ij} X_i X_j \quad (1)$$

Here, Y is a dependent variable (rupture strength, size, or sphericity),  $\beta_0$  is a constant,  $\beta_i$ ,  $\beta_{ii}$ ,  $\beta_{ij}$  are regression coefficients,  $X_i$  and  $X_j$  are levels of the independent variables. The target value of Y<sub>1</sub> maximum and response optimization were calculated by the response optimizer in the MINITAB software. Three-dimensional response surface plots were developed using Maple software (Version 7, Waterloo Maple Inc., Waterloo, Ontario, Canada) and represented a function of two independent variables.

## 7. Scanning electron microscopy (SEM)

To investigate the influence of heat treatment on CAG bead microstructure, the CAG beads were immersed in liquid nitrogen and cut with a knife to obtain the cross section. The CAG beads then underwent lyophilization in a freeze-dryer (CoolSafe, Lynge, Denmark) for 24 h. Moreover, the CAG beads were fixed to a sample with a gold layer using an ion sputter device (Hitachi, E-1010, Tokyo, Japan), and viewed by SEM (JSM-6490LV, JEOL Ltd., Tokyo, Japan) at an accelerating voltage of 15 kV.

## 8. Weight and water contents of the CAG beads

Water content (%) was measured with a moisture analyzer (MX-50, A&D, Tokyo, Japan). The CAG beads were weighed and placed on the analyzer and heated at 100 °C until no weight change was observed. The difference between the original and final weight was considered as the water content. Weighing was performed on a digital balance (Model Radwag, AS 220-R1, Radom, Poland). Water content and weight are expressed as the mean of three replications.

## 9. Measurement of density

The mean weights and diameters of the beads were measured and used to calculate densities of beads using the following Equation (2):

$$D = \frac{M}{V}, \text{ and } V = \frac{4}{3} \pi r^3 \quad (2)$$

where D is the density of the beads; M is the weight of the beads; V is the volume of the beads; r is the radius of the beads.

# Results and Discussion

## 1. Diagnostic checking of the fitted models

Table 2 presents the experimental design and values of the dependent variables considering different heat treatment conditions. It is necessary to fit the quadratic polynomial equation to describe the behavior of the dependent variables on independent variables [15]. Response surface model equations are estimated by a statistical approach called the least-squares technique [16]. The fitted response surface model equations are shown in Table 3. The determination coefficient ( $R^2$ ) value indicates that the model equations described the experimental designs adequately [17]. In general, the more suitable the consideration of the lowest standard deviation, the highest  $R$ -squared values ( $R^2$ , adjusted  $R^2$ ), the better the fit [18]. A  $p$ -value smaller than 0.05 implies that the corresponding model term is significant [19]. The  $R^2$  values of  $Y_1$  (rupture strength),  $Y_2$  (size), and  $Y_3$  (sphericity) were 0.904, 0.888 ( $p < 0.05$ ), and 0.935 ( $p < 0.01$ ), respectively. The statistical significance of the quadratic polynomial model equation was evaluated by analysis of variance (ANOVA), shown in Table 4; the results for the models show the response of the three dependent variables. The results of the lack of fit test, which indicates the fitness of the model [20], showed that the  $F$ -values of  $Y_1$ ,  $Y_2$ , and  $Y_3$  were 9.57, 8.63, and 1.57, respectively; the related  $p$ -values were not significant (0.096, 0.106, and 0.412, respectively) ( $p > 0.05$ ). These results indicate that the models were suitable for accurately predicting variation [21].

**Table 2. Central composite design matrix and values of dependent variables for monitoring the effects of thermal treatment on physical properties of CAG beads.**

Run No.	Independent variables				Dependent variables			
	Coded values		Uncoded values		Y <sub>1</sub>	Y <sub>2</sub>	Y <sub>3</sub>	
	X <sub>1</sub>	X <sub>2</sub>	X <sub>1</sub>	X <sub>2</sub>				
Factorial portions	1	-1	-1	49	13.1	2658	2.73	96.6
	2	1	-1	91	13.1	3692	2.31	95.6
	3	-1	1	49	52	2243	2.73	96.6
	4	1	1	91	52	3516	2.28	95.5
Axial portions	5	-1.414	0	40	32.5	2597	2.62	96.0
	6	1.414	0	100	32.5	3408	2.28	95.4
	7	0	-1.414	70	5	3244	2.46	97.6
	8	0	1.414	70	60	2773	2.44	96.7
Center points	9	0	0	70	32.5	3060	2.48	98.0
	10	0	0	70	32.5	3177	2.43	98.2
	11	0	0	70	32.5	3032	2.49	98.7

X<sub>1</sub>: Heating temperature (°C), X<sub>2</sub>: Heating time (min). Y<sub>1</sub>: Rupture strength (kPa), Y<sub>2</sub>: size (mm), Y<sub>3</sub>: sphericity (%).

**Table 3. Response surface model equations for monitoring the effects of thermal treatment on physical properties of CAG beads**

Quadratic polynomial model equations	$R^2$	$p$ -value
$Y_1 = 3090 + 431.7 X_1 - 157.1 X_2 - 38.1 X_1^2 - 35.1 X_2^2 + 59.8 X_1 X_2$	0.904	0.014
$Y_2 = 2.34667 - 0.1689 X_1 - 0.0073 X_2 - 0.0073 X_1^2 - 0.0073 X_2^2 - 0.0075 X_1 X_2$	0.888	0.020
$Y_3 = 98.300 - 0.369 X_1 - 0.172 X_2 - 1.388 X_1^2 - 0.663 X_2^2 - 0.025 X_1 X_2$	0.935	0.005

$X_1$ : Heating temperature ( $^{\circ}\text{C}$ ),  $X_2$ : Heating time (min).  $Y_1$ : Rupture strength (kPa),  $Y_2$ : size (mm),  $Y_3$ : sphericity (%).

**Table 4. Analysis of variance for dependent variables**

Dependent variables	Sources	DF	SS	MS	F-value	p-value
Y <sub>1</sub> Rupture strength (kPa)	Regression					
	Linear	2	1688737	844369	23.23	0.003
	Square	2	11756	5878	0.16	0.855
	Interaction	1	14280	14280	0.39	0.558
	Residual					
	Lack of fit	3	169872	56624	9.57	0.096
	Pure error	2	11833	5916		
	Total	10	1896479			
Y <sub>2</sub> Size (mm)	Regression					
	Linear	2	0.228518	0.114259	19.83	0.004
	Square	2	0.000464	0.000232	0.04	0.961
	Interaction	1	0.000225	0.000225	0.04	0.851
	Residual					
	Lack of fit	3	0.026744	0.008915	8.63	0.106
	Pure error	2	0.002067	0.001033		
	Total	10	0.258018			
Y <sub>3</sub> Sphericity (%)	Regression					
	Linear	2	1.3223	0.6611	3.79	0.100
	Square	2	11.2716	5.6358	32.29	0.001
	Interaction	1	0.0025	0.0025	0.01	0.909
	Residual					
	Lack of fit	3	0.6127	0.2042	1.57	0.412
	Pure error	2	0.2600	0.1300		
	Total	10	13.4691			

DF: Degrees of freedom, SS: Sum of square, MS: Mean square.

## 2. Response surface plots and the effect of factors

Table 5 provides the calculated data for significance with t-statistic and the estimated coefficients of the linear ( $X_1$ ,  $X_2$ ), quadratic ( $X_1X_1$ ,  $X_2X_2$ ), and interaction ( $X_1X_2$ ) terms for the three dependent variables ( $Y_1$ ,  $Y_2$ , and  $Y_3$ ). The effects of heating temperature ( $X_1$ ) and heating time ( $X_2$ ) on rupture strength ( $Y_1$ ), size ( $Y_2$ ), and sphericity ( $Y_3$ ) are expressed as a three-dimensional plot (Figure 2). The larger t-value and smaller p-value indicate the significance of parameters [22].

The rupture strength ( $Y_1$ ) increased when the heating temperature ( $X_1$ ) increased from 40 °C (-1.414) to 100 °C (+1.414);  $Y_1$  decreased when heating time ( $X_2$ ) increased from 5 min (-1.414) to 60 min (+1.414) (Figure 2a). The linear term for  $Y_1$  was significant ( $p < 0.01$ ), while their square terms and interaction terms were not significant ( $p > 0.05$ ) (Table 4). The  $X_1$  term for  $Y_1$  was significant ( $p < 0.01$ ), while the  $X_2$  term for  $Y_1$  was not significant ( $p > 0.05$ ) (Table 5). We found that the heating temperature ( $X_1$ ) is a significant factor affecting the rupture strength ( $Y_1$ ); however, there was no statistically significance between rupture strength ( $Y_1$ ) and heating time ( $X_2$ ). This result supports previous research [23], which studied the effect of temperature on the structure of calcium alginate beads. This study shows that the comparison of the mechanical resistance at different temperatures (80, 110, and 130 °C), for the same period (0, 5, 10, 15, and 20 min) of incubation, shows that a higher resistance is always obtained at the higher temperature. A previous study also reported that hardness of the alginate-guar gels mixed with pimiento pulp significantly increased when applying thermal treatment (80 °C for 15 min) [24]. The authors reported that the increase in hardness of the alginate-guar gels originated from the occurrence of gel shrinkage, making them more compact during heat treatment [24].

The size ( $Y_2$ ) sharply decreased with an increase in the heating temperature ( $X_1$ ) from 40 °C (-1.414) to 100 °C (+1.414); however, there was no significant relationship between size ( $Y_2$ ) and heating time ( $X_2$ ) from 5 min (-1.414) to 60 min (+1.414) ( $p > 0.05$ ) (Figure 2b). The linear terms for  $Y_2$  were significant ( $p < 0.01$ ), while their square terms and interaction terms were not significant ( $p > 0.05$ ) (Table 4). The  $X_1$  term for  $Y_2$  was significant ( $p < 0.01$ ), while  $X_2$  term for  $Y_2$  was not significant ( $p > 0.05$ ) (Table 5). Here, it is apparent heating temperature ( $X_1$ ) is a significant factor affecting the size ( $Y_2$ ); however, there was no significant relationship between the size ( $Y_2$ ) and heating time ( $X_2$ ). This finding is consistent with previous study results [25], where the average bead size, after 30 min of heat treatment (90 °C), was showing 0.3 mm (3.62 mm to 3.32 mm) of shrinkage. Likewise, other authors [23] found that the reduction in bead size clearly depends on both time (0, 5, 10, 15, and 20 min) and temperature (80, 110, and 130 °C). The size reduction may be related to water loss [26-28]. As the CAG beads were heated, there was a greater amount of water exuded and therefore, greater the size reduction.

The sphericity ( $Y_3$ ) increased as the coded values of independent variables approached zero (Figure 2c). The linear and interaction terms for  $Y_3$  were not significant ( $p > 0.05$ ), while their square terms were significant ( $p < 0.01$ ) (Table 4). The linear and interaction terms for  $Y_3$  were not significant a ( $p > 0.05$ ), while their square terms were significant ( $p < 0.01$ ) (Table 5). Previous authors [7] found that caviar analogs using CAG had sphericities ranging from 90 to 100%, measured with a digital microscope, and could not be differentiated with the naked eye. In Figure 2, the CAG beads after heat treatment from 40 °C (-1.414) to 100 °C (+1.414) showed sphericities ranging from 94% to 97%. We believe, therefore, that the change of heating temperature and heating time did not significantly affect the sphericity of the CAG

beads, as they retained their spheroid shape.

In conclusion, the rupture strength ( $Y_1$ ) and size ( $Y_2$ ) affected dependent variables, with heating temperature ( $X_1$ ) being the most important factor. In addition, as the CAG beads' heating temperature ( $X_1$ ) increased, the rupture strength ( $Y_1$ ) increased and the size ( $Y_2$ ) decreased.



**Table 5. Estimated coefficients of the fitted quadratic polynomial equations for dependent variables based on the *t*-statistic**

Parameters	Y <sub>1</sub>		Y <sub>2</sub>		Y <sub>3</sub>	
	Rupture strength (kPa)		Size (mm)		Sphericity (%)	
	Coefficient	<i>p</i> -value	Coefficient	<i>p</i> -value	Coefficient	<i>p</i> -value
Constant	3090	0.001	2.4667	0.001	98.300	0.001
X <sub>1</sub>	431.7	0.001	-0.1689	0.001	-0.369	0.055
X <sub>2</sub>	-157.1	0.067	-0.0073	0.797	-0.172	0.298
X <sub>1</sub> X <sub>1</sub>	-38.1	0.654	0.0073	0.828	-1.388	0.001
X <sub>2</sub> X <sub>2</sub>	-35.1	0.680	0.0073	0.828	-0.663	0.013
X <sub>1</sub> X <sub>2</sub>	59.8	0.558	-0.0075	0.851	-0.025	0.909

X<sub>1</sub>: Heating temperature (°C), X<sub>2</sub>: Heating time (min).

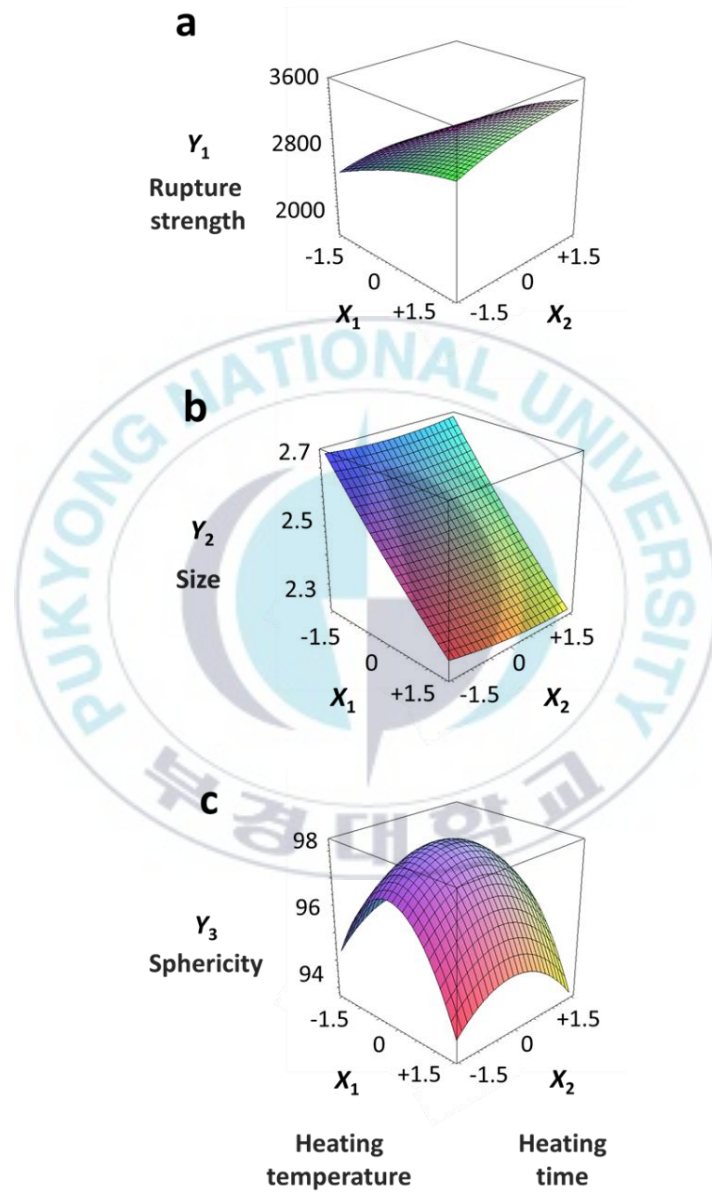
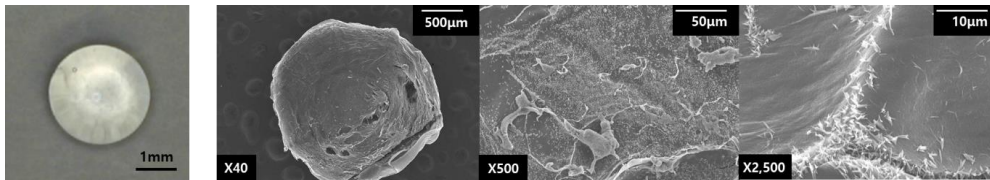


**Figure 2. Three-dimensional response surface plots for rupture strength (a), size (b), and sphericity (c). X<sub>1</sub>; Heating temperature (°C), X<sub>2</sub>; Heating time (min).**

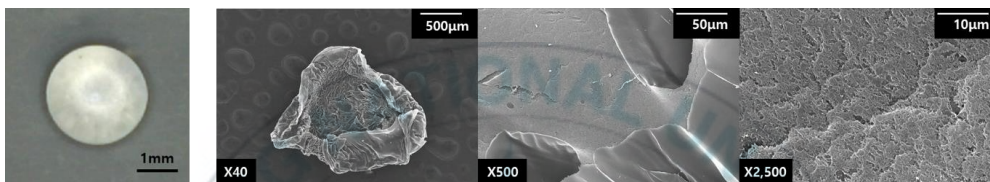
### 3. Microstructure

To better understand the effects of heat treatment on physical properties of CAG beads, we analyzed the microstructure of the CAG beads through SEM image. For this, freeze-dried CAG beads were used and were compared with CAG beads heated at 40, 70, and 100 °C (Figure 3). Digital microscope observations showed that in both the unheated and heated tests, the CAG beads retained their spheroid shape. However, the freeze-dried CAG beads did not retain their spheroid shape. We believe that the water loss during freeze-drying involves shrinkage and deformation of CAG beads dimension, which increases the particle density [29]. The CAG beads after heat treatment presented an altered structure when compared to unheated CAG beads' structure. Unheated CAG beads are homogeneous and smooth (Figure 3a) because they did not lose water. Conversely, after heat treatment, the CAG beads have a greater porous structure (Figure 3b-d) because they lost water. When the heating temperature ( $X_1$ ) increased from 70 °C to 100 °C, the CAG beads gradually formed a more compact gel network with a homogeneous distribution of small pores, while the CAG beads, after heat treatment at 40 °C exhibited void pores. The change of microstructure in the CAG beads could explain the change in physical properties. Our findings revealed that at higher temperatures, the rupture strength increased (Table 2). This indicates that water loss leads to a more dense porous structure, thus increasing rupture strength. In Table 6, the density of unheated CAG beads and that of heated CAG beads at 40, 70, and 100 °C was calculated. These findings provide evidence that the increase in rupture strength was due to an increase in the density [30]. A similar microstructure was observed previously [31] and a higher strength of gel microstructure was more uniform and continuous with smaller voids.

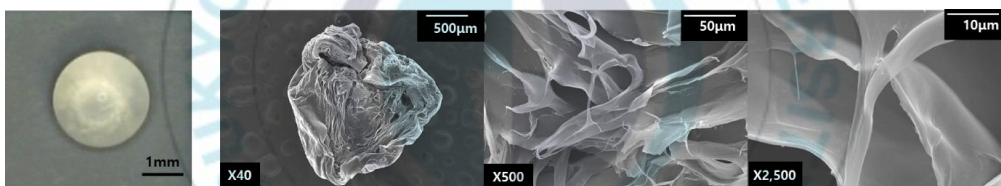
a) Non-heated CAG beads



b) Heated CAG beads at 40°C



c) Heated CAG beads at 70°C



d) Heated CAG beads at 100°C

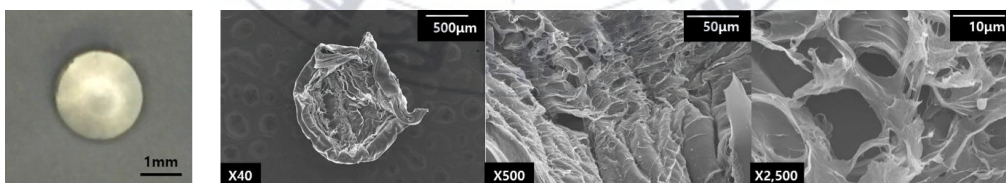


**Figure 3. Digital microscope (left), and SEM (right) photographs of CAG beads frozen in liquid nitrogen and freeze-dried: (a) before heat treatment CAG bead; (b) CAG beads were heated at 40 °C; (c) CAG beads were heated at 70 °C; (d) CAG beads were heated at 100 °C. Magnification of the images are 40×, 500×, and 2500×.**

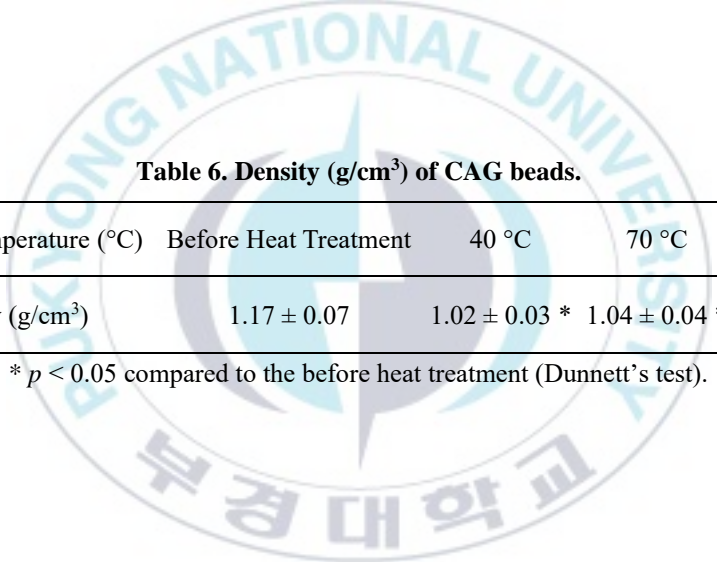


**Table 6. Density (g/cm<sup>3</sup>) of CAG beads.**

Heating Temperature (°C)	Before Heat Treatment	40 °C	70 °C	100 °C
Density (g/cm <sup>3</sup> )	1.17 ± 0.07	1.02 ± 0.03 *	1.04 ± 0.04 *	1.26 ± 0.05

\*  $p < 0.05$  compared to the before heat treatment (Dunnett's test).

Heating at 70 and 100 °C significantly reduced the CAG bead size believed to result from water loss [26-28]. Thus, we believe that syneresis, a phenomenon whereby water molecules are exuded out of a gel matrix because of an external force that contracts the gel, occurs when treated with heat [11, 32]. We investigated whether this size reduction was correlated to water leakage, water content, size, and weight of the CAG beads after heat treatment at 40, 70, and 100 °C for 5 min to 32.5 min (Figure 4). The size ( $Y_2$ ) and weight were correlated ( $R^2 = 0.921, 0.946$ ). Here, data shows that the higher the heated temperature of the CAG beads, the more significant size ( $Y_2$ ) and weight reduction. Moreover, size ( $Y_2$ ) and water content were correlated ( $R^2 = 0.911, 0.798$ ). However, the water content of the CAG beads decreased as the heat treatment increased. The weight of the non-heated CAG beads was 11.5 mg and the weight of the heated CAG beads at 100 °C was 5.8 mg. The water content of the non-heated CAG beads was 95.9%, while that of the CAG beads heated at 100 °C was 93.3%. Our findings reveal that the absolute water content 11.03 mg was reduced to 5.39 mg and there was a 51.2% water loss.

In conclusion, the SEM images, with the water content, weight, and size correlations show that the denser the structure of the CAG beads after exposure to higher heating temperatures, the less available space there is for water, resulting in increased rupture strength and reduced size.

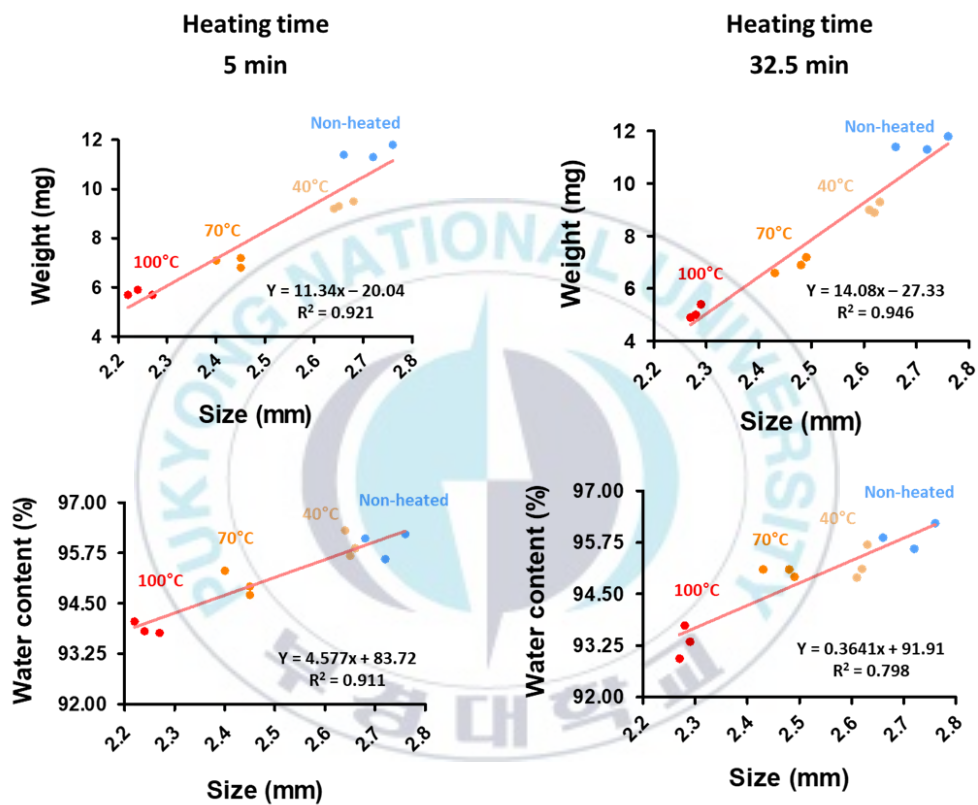


Figure 4. Correlation between weight (mg) and size (mm), water content (%) and size (mm) at 5 min; and weight (mg) and size (mm), water content (%) and size (mm) at 32.5 min.

#### 4. Optimal conditions and verification

In the food industry, it is recommended that minimum changes occur in foods prepared with CAG during thermal processes such as sterilization, cooking, and manufacturing. Therefore, in this study, three optimized heat-treated CAG beads were prepared to give similar results as non-heated CAG beads considering the rupture strength ( $Y_1$ ), size ( $Y_2$ ), and sphericity ( $Y_3$ ) and were verified (Table 7). The optimal conditions, including the coded and uncoded values of the independent variables, are shown in Table 8. The optimal conditions indicated the rupture strength ( $Y_1$ ), size ( $Y_2$ ), and sphericity ( $Y_3$ ) of the unheated CAG beads were  $3450 \pm 112.47$  kPa,  $2.60 \pm 0.05$  mm, and  $96.5 \pm 2.14\%$ , respectively. According to the results of CCD, the optimal conditions of  $X_1$  (heating temperature) and  $X_2$  (heating time) were  $-0.6649$  ( $56.0371$  °C) and  $-1.414$  (5 min), respectively. To facilitate the operation, the optimal process conditions of heating time and temperature were  $56$  °C and 5 min, respectively. The predicted values of  $Y_1$ ,  $Y_2$ , and  $Y_3$  for each optimal condition were 2993 kPa, 2.60 mm, and 96.8%, respectively. To verify the accuracy of the predicted  $Y_1$ ,  $Y_2$ , and  $Y_3$  values, the CAG beads were prepared under each of the optimal conditions and tested. The experimental values of  $Y_1$ ,  $Y_2$ , and  $Y_3$  were  $2844 \pm 66.64$  kPa,  $2.55 \pm 0.02$  mm, and  $96.0 \pm 2.25\%$ , respectively, similar to the predicted values (Table 9).

**Table 7. The rupture strength, size, and sphericity of before heat treatment CAG beads.**

	Y <sub>1</sub> Rupture Strength (kPa)	Y <sub>2</sub> Size (mm)	Y <sub>3</sub> Sphericity (%)
Before heat treatment	3450 ± 112.50	2.60 ± 0.05	96.5 ± 2.15

**Table 8. Response optimization for processing a heated CAG beads similar result to non-heated CAG beads conditions**

Optimal conditions	X <sub>1</sub>		X <sub>2</sub>		
	Heating temperature (°C)		Heating time (min)		
	Coded value	Actual value	Coded value	Actual value	
	-0.665	56.0	-1.414	5	
Y <sub>1</sub> Rupture strength (kPa)	Target value				
	3450 kPa				
Y <sub>2</sub> Size (mm)	Target value				
	2.60 mm				
Y <sub>3</sub> Sphericity (%)	Target value				
	96.5%				

**Table 9. Experimental and predicted results of verification under optimized conditions**

	Y <sub>1</sub> Rupture strength (kPa)	Y <sub>2</sub> Size (mm)	Y <sub>3</sub> Sphericity (%)
Predicted values	2993	2.60	96.8
Experimental values	2844 ± 66.64	2.55 ± 0.02	96.0 ± 2.25

Optimized conditions: heating temperature = 56 °C; heating time = 5 min.

## Conclusions

Calcium alginate gel (CAG) is used to make artificial or imitative foods because of its unique gelling abilities and is a promising biomaterial in the food industry. In the food industry, it is important to verify stability and process suitability for artificial or imitative foods using CAG; the effects of heat treatment on the physical properties of CAG beads can be utilized in several ways. Our findings reveal that the heating temperature ( $X_1$ ) was the factor that had the greatest effect on the rupture strength ( $Y_1$ ) and size ( $Y_2$ ). The CAG beads increased in rupture strength and decreased in size as the heating temperature increased because of water loss. RSM was successfully employed to optimize the non-heated CAG beads. Under each optimal condition,  $Y_1$ ,  $Y_2$ , and  $Y_3$  were  $2844 \pm 66.64$  kPa,  $2.55 \pm 0.02$  mm, and  $96.0 \pm 2.25\%$ , respectively. Our results indicate that the heat treatment of CAG can be used not only for sterilization and cooking but also as a processing technique by controlling the physical properties.

## References

1. Leong, J.Y.; Lam, W.H.; Ho, K.W.; Voo, W.P.; Lee, M.F.X.; Lim, H.P.; Lim, S.L.; Tey, B.T.; Poncelet, D.; Chan, E.S. Advances in Fabricating Spherical Alginate Hydrogels with Controlled Particle Designs by Ionotropic Gelation as Encapsulation Systems. *Particuology* 2016, 24, 44–60.
2. Tavassoli-Kafrani, E.; Shekarchizadeh, H.; Masoudpour-Behabadi, M. Development of Edible Films and Coatings from Alginates and Carrageenans. *Carbohydr. Polym.* 2016, 137, 360–374.
3. Yang, J.S.; Xie, Y.J.; He, W. Research Progress on Chemical Modification of Alginate: A Review. *Carbohydr. Polym.* 2011, 84, 33–39.
4. Lopez-Sanchez, P.; Fredriksson, N.; Larsson, A.; Altskär, A.; Ström, A. High Sugar Content Impacts Microstructure, Mechanics and Release of Calcium-Alginate Gels. *Food Hydrocoll.* 2018, 84, 26–33.
5. Zactiti, E.M.; Kieckbusch, T.G. Potassium Sorbate Permeability in Biodegradable Alginate Films: Effect of the Antimicrobial Agent Concentration and Crosslinking Degree. *J. Food Eng.* 2006, 77, 462–467.
6. Lee, K.Y.; Mooney, D.J. Alginate: Properties and Biomedical Applications. *Prog. Polym. Sci.* 2012, 37, 106–126.
7. Ji, C.; Cho, S.; Gu, Y.; Kim, S. The Processing Optimization of Caviar Analogs Encapsulated by Calcium-Alginate Gel Membranes. *Food Sci. Biotechnol.* 2007, 16, 557–564.
8. Ha, B.B.; Jo, E.H.; Cho, S.; Kim, S.B. Production Optimization of Flying Fish Roe Analogs Using Calcium Alginate Hydrogel Beads.

Fish. Aquat. Sci. 2016, 19, 1–7.

9. Roh, H.-J.; Jo, E.-H.; Kim, H.-D.; Kim, S.-B. Effects of Physicochemical Parameters on Production of Cooked Rice Analogs by Calcium Alginate Gels. *Korean J. Fish. Aquat. Sci.* 2016, 49, 20–25.
10. Madoumier, M.; Trystram, G.; Sébastien, P.; Collignan, A. Towards a holistic approach for multi-objective optimization of food processes: A critical review. *Trends Food Sci. Tech.* 2019, 86, 1–15.
11. Ching, S.H.; Bansal, N.; Bhandari, B. Alginate gel particles—A review of production techniques and physical properties. *Crit. Rev. Food Sci. Nutr.* 2017, 57, 1133–1152.
12. Erbay, Z.; Icier, F. Optimization of hot air drying of olive leaves using response surface methodology. *J. Food Eng.* 2009, 91, 533–541.
13. Jancy, S.; Shruthy, R.; Preetha, R. Fabrication of packaging film reinforced with cellulose nanoparticles synthesised from jack fruit non-edible part using response surface methodology. *Int. J. Biol. Macromol.* 2019. In press.
14. Said, K.A.M.; Amin, M.A.M. Overview on the response surface methodology (RSM) in extraction processes. *J. Appl. Sci. Process Eng.* 2015, 2.
15. Bezerra, M.A.; Santelli, R.E.; Oliveira, E.P.; Villar, L.S.; Escalera, L.A. Response Surface Methodology (RSM) as a Tool for Optimization in Analytical Chemistry. *Talanta* 2008, 76, 965–977.
16. Ba, D.; Boyaci, I.H. Modeling and Optimization i: Usability of Response Surface Methodology. *J. Food Eng.* 2007, 78, 836–845.
17. Cho, S.M.; Gu, Y.S.; Kim, S.B. Extracting Optimization and Physical Properties of Yellowfin Tuna ( *Thunnus Albacares* ) Skin Gelatin Compared to Mammalian Gelatins. *Food Hydrocoll.* 2005, 19, 221–229.
18. Shishir, M.R.I.; Taip, F.S.; Aziz, N.A.; Talib, R.A.; Sarker, M.S.H. Optimization of spray drying parameters for pink guava powder using RSM. *Food Sci. Biotechnol.* 2016, 25, 461–468.

19. Noshadi, I.; Amin, N.A.S.; Parnas, R.S. Continuous production of biodiesel from waste cooking oil in a reactive distillation column catalyzed by solid heteropolyacid: Optimization using response surface methodology (RSM). *Fuel* 2012, 94, 156–164.
20. Isa, K.M.; Daud, S.; Hamidin, N.; Ismail, K.; Saad, S.A.; Kasim, F.H. Thermogravimetric Analysis and the Optimisation of Bio-Oil Yield from Fixed-Bed Pyrolysis of Rice Husk Using Response Surface Methodology (RSM). *Ind. Crops. Prod.* 2011, 33, 481–487.
21. Bimakr, M.; Rahman, R.A.; Ganjloo, A.; Taip, F.S.; Salleh, L.M.; Sarker, M.Z.I. Optimization of Supercritical Carbon Dioxide Extraction of Bioactive Flavonoid Compounds from Spearmint (*Mentha Spicata* L.) Leaves by Using Response Surface Methodology. *Food Bioprocess Tech.* 2012, 5, 912–920.
22. Bahrani, S.; Razmi, Z.; Ghaedi, M.; Asfaram, A.; Javadian, H. Ultrasound-accelerated synthesis of gold nanoparticles modified choline chloride functionalized graphene oxide as a novel sensitive bioelectrochemical sensor: Optimized meloxicam detection using CCD-RSM design and application for human plasma sample. *Ultrason. Sonochem.* 2018, 42, 776–786.
23. Serp, D.; Mueller, M.; Stockar, U. Von; Marison, I.W. Low-Temperature Electron Microscopy for the Study of Polysaccharide Ultrastructures in Hydrogels. II. Effect of Temperature on the Structure of Ca<sup>2+</sup>-Alginate Beads. *Biotechnol. Bioeng.* 2002, 79, 253–259.
24. Mousavi, S.M.R.; Rafe, A.; Yeganehzad, S. Textural, Mechanical, and Microstructural Properties of Restructured Pimiento Alginate-Guar Gels. *J. Texture Stud.* 2019, 50, 155–164.
25. Woo, J. W.; Roh, H. J.; Park, H. D.; Lee, Y. B.; Kim, S. B.; Ji, C. I. Sphericity Optimization of Calcium Alginate Gel Beads and the Effects of Processing Conditions on Their Physical Properties. *Food Sci. Biotechnol.* 2007, 16, 715–721.

26. Singh, D.; Tripathi, A.; Zo, S.M.; Singh, D.; Han, S.S. Synthesis of Composite Gelatin-Hyaluronic Acid-Alginate Porous Scaffold and Evaluation for in Vitro Stem Cell Growth and in Vivo Tissue Integration. *Colloids Surf. B* 2014, 116, 502–509.
27. Zohuriaan, M.J.; Shokrolahi, F. Thermal Studies on Natural and Modified Gums. *Polym. Test.* 2004, 23, 575–579.
28. Yang, H.; Li, H.; Zhai, J.; Sun, L.; Zhao, Y.; Yu, H. Magnetic Prussian Blue/Graphene Oxide Nanocomposites Caged in Calcium Alginate Microbeads for Elimination of Cesium Ions from Water and Soil. *Chem. Eng. J.* 2014, 246, 10–19.
29. Vargas, P.O.; Pereira, N.R.; Guimarães, A.O.; Waldman, W.R.; Pereira, V.R. Shrinkage and Deformation during Convective Drying of Calcium Alginate. *LWT Food Sci. Technol.* 2018, 97, 213–222.
30. Sun-Waterhouse, D.; Wang, W.; Waterhouse, G.I. Canola oil encapsulated by alginate and its combinations with starches of low and high amylose content: Effect of quercetin on oil stability. *Food Bioprocess Tech.* 2014, 7, 2159–2177.
31. Mishyna, M.; Martinez, J.J.I.; Chen, J.; Davidovich-Pinhas, M.; Benjamin, O. Heat-Induced Aggregation and Gelation of Proteins from Edible Honey Bee Brood (*Apis Mellifera*) as a Function of Temperature and PH. *Food Hydrocoll.* 2019, 91, 117–126.
32. Roopa, B.S.; Bhattacharya, S. Alginate Gels: Ii. Stability at Different Processing Conditions. *J. Food Process Eng.* 2010, 33, 466–480.

## **Publications and Presentations**

### **Publications**

Kim, S.; Jeong, C.; Cho, S.; Kim, S. B. Effects of Thermal Treatment on the Physical Properties of Edible Calcium Alginate Gel Beads: Response Surface Methodological Approach. *Foods* 2019, 8, 578.

### **Oral presentations**

May 9. 2019. Korean Federation of Fisheries Science and Technology Societies (in Korea)

Title: Changes on physical properties of calcium alginate gel beads after thermal treatment: Response surface methodological approach

### **Poster presentations**

1. November 2. 2018. Korean Federation of Fisheries Science and Technology Societies International Conference (in Korea)

Title: Monitoring and optimization of physical properties of calcium alginate gel beads during heat treatment using response surface methodology

2. October 24. 2019. The Korean Society of Food Science and Nutrition International Symposium and Annual Meeting (in Korea)

Title: Effects of thermal treatment on physical properties of calcium alginate gel beads

## Acknowledgments

어느새 길다면 길고 짧다면 짧은 석사과정을 마치고 학위 논문을 제출하게 되었습니다. 지난 시간 동안 부족한 점이 많은 저에게 도움을 주신 분들이 많습니다. 미흡하지만 학위 논문을 마치면서 그분들께 감사의 말씀 전합니다.

우선 항상 따뜻한 마음으로 큰아버지처럼 챙겨 주시고 좋은 말씀과 연구를 올바른 방향으로 이끌어 주신 김선봉 지도 교수님께 감사합니다. 교수님 덕분에 학부 2학년 때부터 실험실에 들어와 잊지 못할 추억과 다양한 연구를 배울 수 있었습니다.

그리고 언제나 모르는 것이 있어 찾아가면 학교 선배님처럼 친근하게 해답을 제시해 주신 조승목 교수님께도 감사합니다. 교수님 덕분에 값진 경험들을 많이 할 수 있었으며 교수님 옆에서 배우면서 졸업을 한 후 연구를 계속하고 싶게 되었습니다.

다시 한번 두 분의 교수님께 감사드리며 가르침에 부끄럽지 않게 최선을 다하겠습니다.

또한 학부와 석사과정에서 많은 가르침을 주신 양지영 교수님, 전병수 교수님, 이양봉 교수님, 안동현 교수님, 김영목 교수님께 감사의 마음 전합니다.

식품화학실험실에서 가장 오랜 시간을 함께 하고 같이 연구하면서 동기부여가 되어준 착해서 걱정이 많은 충은 선배, 푸근한 투덜이 도훈 선배, 둘째 오빠 같은 찬민 선배, 친구처럼 장난 잘 받아 주는 마음 어린 랩장 기범 선배, 5년 동안 장난 받아주고 있는 고마운 희라, 하면 한다 재석 선배, 실험실에 늦게 들어와 적응하는데 힘들었겠지만 잘 해주고 있는 소현이, 지연이, 항상 응원해주고 웃게 해주는 둘도 없는 15학번 동기 지호, 종민,

학부장으로써 든든한 동민 선배, 언니로써 많이 못 챙겨줘서 미안한 귀염둥이 정윤, 윤진, 수빈, 나을, 장난 많이 쳐줘서 고마운 막내 원석이까지 모두 많은 힘이 되었고 덕분에 석사 생활을 행복하게 마무리할 수 있었습니다. 정말 감사하다는 말을 전하고 싶습니다.

마지막으로 언제나 옆에서 믿어 주시고 응원해 주시고 말로는 표현을 잘 못해 죄송한 부모님께 감사한 마음을 전합니다. 꼭 성공해서 보답하겠습니다. 감사합니다.

